Rock Mech Rock Eng (2017) 50:3233–3244
https://doi.org/10.1007/s00603-017-1297-9

ORIGINAL PAPER

Determination of Destress Blasting Effectiveness Using Seismic Source Parameters

Łukasz Wojtecki[1] · **Maciej J. Mendecki**[2] · **Wacaław M. Zuberek**[2]

Received: 5 October 2016 / Accepted: 9 August 2017 / Published online: 24 August 2017

Abstract Underground mining of coal seams in the Upper Silesian Coal Basin is currently performed under difficult geological and mining conditions. The mining depth, dislocations (faults and folds) and mining remnants are responsible for rockburst hazard in the highest degree. This hazard can be minimized by using active rockburst prevention, where destress blastings play an important role. Destress blastings in coal seams aim to destress the local stress concentrations. These blastings are usually performed from the longwall face to decrease the stress level ahead of the longwall. An accurate estimation of active rockburst prevention effectiveness is important during mining under disadvantageous geological and mining conditions, which affect the risk of rockburst. Seismic source parameters characterize the focus of tremor, which may be useful in estimating the destress blasting effects. Investigated destress blastings were performed in coal seam no. 507 during its longwall mining in one of the coal mines in the Upper Silesian Coal Basin under difficult geological and mining conditions. The seismic source parameters of the provoked tremors were calculated. The presented preliminary investigations enable a rapid estimation of the destress blasting effectiveness using seismic source parameters, but further analysis in other geological and mining conditions with other blasting parameters is required.

✉ Maciej J. Mendecki
maciej.mendecki@us.edu.pl

[1] Polish Mining Group, ul. Powstańców 30, 40-039 Katowice, Poland

[2] Faculty of Earth Sciences, University of Silesia in Katowice, ul. Bedzisnska 60, 41-200 Sosnowiec, Poland

Keywords Active rockburst prevention · Destress blasting · Seismic source parameters

1 Introduction

Rockburst is a dangerous dynamic catastrophic phenomenon that occurs during deep underground coal mining in the Upper Silesian Coal Basin (USCB). Rockburst is associated with the destruction or loss of functionality of the excavations. To reduce the rockburst hazard, both passive and active rockburst preventions are applied. Several rockburst prevention techniques have been developed over many years. In the active rockburst prevention, long-hole destress blasting (i.e. torpedo blasting) in the roof rocks plays an important role. The main purpose of these blastings is to reduce stress concentrations in the rock mass and fracture the thick layers of strong roof rocks to prevent or minimize the effect of high-energy tremors on the excavations or reduce the seismic hazard. It is important to achieve a new, more advantageous equilibrium state in the rock mass via destress blasting. Parameters of the destress blasting are established according to the geological and mining conditions and the technological opportunities.

Estimation of the destress blasting effectiveness, which is correlated with the seismic activity and high probability of rockburst, is particularly important during mining in difficult geological and mining conditions. At present, the seismic energy of provoked tremor is the main parameter to estimate the destress blasting effectiveness in hard coal mines (e.g. Konicek et al. 2013; Wojtecki and Konicek 2016).

The focus of a tremor can be characterized by seismic source parameters such as the size of the focus and the state of stress in the focus. Seismic source parameters also describe the strength of the tremor. Seismic source

parameters are usually determined for naturally occurring seismic events or mining-induced tremors, but they can also be determined for tremors provoked by the destress blasting. Seismic source parameters cannot be excluded as a useful tool for the estimation of the effectiveness and seismic energy of the long-hole destress blasting in the roof rocks. In the foci of provoked tremors, an explosion predominates, but other processes may also occur, such as a slip mechanism and an implosion (Wojtecki et al. 2013). The occurrence of additional processes is associated with the new equilibrium state in the rock mass. In this case, the destress of the rock mass increases, and fracturing that is not solely related to the detonation of the explosives is present.

We attempt to determine the seismic source parameters of tremors provoked by the long-hole destress blasting stages in the roof rocks during the longwall mining of coal seam no. 507 in a hard coal mine in the Polish part of the USCB in the region of the main saddle. The effectiveness of destress blasting is estimated.

2 Geological and Mining Conditions

Coal seam no. 507 in the region of the selected longwall is deposited at a depth of 870–910 m below the ground level. Its thickness is 2.7–3.8 m, and its inclination is 2°–10°. The direct roof of coal seam no. 507 is composed of alternating layers of shale, sandy shale and sandstone (Fig. 1). Most of these rocks are tough with a high uniaxial compressive strength R_C (17–85 MPa; mean value: 55 MPa). At a distance of more than 50 m above coal seam no. 507, there is a thick layer (up to 60 m) of sandstone ($R_C = 80$ MPa). There are a shale layer and a sandy shale layer in the floor of coal seam no. 507, whose thickness is small (several metres), and the thick coal seam no. 510 (up to 8 m) is deposited below (Fig. 1).

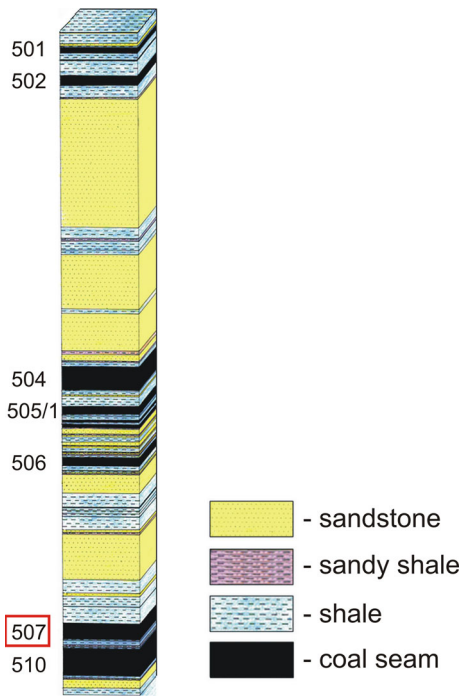

Fig. 1 Lithological structure of the rock mass in the area of the selected longwall (Wojtecki et al. 2016)

Coal seam no. 507 with the selected longwall was extracted from January 2011 to June 2012. The longwall began near the protecting pillar for the flank drifts. There is an abandoned goaf in the upper stage to the north of the selected longwall. At the end, the longwall approached the protecting pillars for the shaft and main drifts.

In the area of the selected longwall, coal seams nos. 501 and 502 (approximately 150 and 135 m above coal seam no. 507) were extracted earlier (Fig. 1). This extraction was not clean and created mining edges, which are boundaries of exploitation in coal seams and increase the stress level in the rock mass. In the middle of the longwall field, these mining edges in coal seams nos. 501 and 502 coexisted and were quasi-parallel to the front of the selected longwall. In this area, the stress concentration in the roof rocks of coal seam no. 507 was extremely high, which is well correlated with the seismic activity.

During underground working in coal seam no. 507 in the past under analogous conditions, without long-hole destress blasting, ten rockbursts occurred. Underground excavations in coal seam no. 507 were destroyed. The in situ stresses in coal seam no. 507 because of the depth of deposition and other geological and mining factors were high (tens of MPa).

3 Rockburst Hazard

The seismic activity in the region of the selected longwall was high, so the rockburst hazard was also high. In total, 6273 tremors were recorded during the mining of coal seam no. 507 with the assigned longwall, and the total released seismic energy was 2.62×10^8 J. Considering low-energy tremors, 3341 tremors had the energy of 10^2 J ($0.11 \leq M_L < 0.63$), and 1840 had the energy of 10^3 J ($0.63 \leq M_L < 1.16$); 897 tremors with the energy of 10^4 J ($1.16 \leq M_L < 1.68$) occurred in the area of the selected longwall. During the longwall mining of coal seam no. 507, 195 high-energy tremors were induced: 160 with the energy of 10^5 J ($1.68 \leq M_L < 2.21$), 34 with the energy of 10^6 J ($2.21 \leq M_L < 2.74$) and the strongest tremor with the energy of 2×10^7 J ($M_L = 2.9$). The tremor energy is calculated in the selected colliery by numerical integration considering the source–seismometer distance, attenuation coefficient and gain of the channel. The presented local

magnitude in brackets was calculated according to the formula of Dubiński and Wierzchowska (1973). The locations of the high-energy tremor sources generated during the longwall mining of coal seam no. 507 are shown in Fig. 2. Monthly longwall face advances (from I 2011 to VI 2012) and axis along the main gate (0–700 m) are shown in Fig. 2.

From August 2011 to March 2012, the level of rockburst hazard in the area of the selected longwall was the highest. Approximately 70% of tremors with the energy of 10^5 J, 97% of tremors with the energy of 10^6 J and the strongest tremor with the energy of 2×10^7 J occurred in this period. At this time, the longwall face was approaching and subsequently running beneath the mining edges in the upper coal seams (nos. 501 and 502) (generally parallel to the longwall face). The induced tremors mostly occurred in front of the longwall face (the average horizontal distance from the longwall face was approximately 90 m). At the foci of the strongest tremors, the shear component predominated, which is likely connected with the fracturing of the thick sandstone layer above coal seam no. 507 (Wojtecki and Dzik 2013). Rock dislocation in the sources of the strongest tremors occurred mainly in the direction of gobs of the selected longwall (Wojtecki and Dzik 2013). The mining edges in coal seams nos. 501 and 502 also affected the occurrence of these tremors (Wojtecki and Dzik 2013). Because of the high seismic activity and associated high level of rockburst hazard, an active rockburst prevention was applied.

4 Active Rockburst Prevention

Active rockburst prevention was mainly based on the destress blasting in the roof rocks of coal seam no. 507. The main purpose of these blasting stages was to destress the rock mass ahead of the longwall face and protect the crew from the effect of high-energy tremors, which were concentrated ahead of the longwall face.

In the first 11 destress blasting stages, six 40-m-long blastholes (arranged in pairs: one pair was in the middle of the longwall face; the other pairs were placed 60 m from the longwall galleries) were performed each time. The blastholes were deviated from the longwall face to the north-east and south-east at an angle of approximately 40° and inclined upwards at an angle of 35° from the horizon. The diameter of each blasthole was 76 mm. The pneumatic loading of blastholes was always applied. The Emulinit PM explosive material was used for each blasting. The explosive material was located among others in the two thickest sandstone layers between coal seams nos. 507 and 506 (Fig. 1). Emulinit PM is produced in cartridges at a minimal diameter of 32 mm and a minimal mass of 300 g (www.nitroerg.pl). This explosive material has a density of 1.15–1.3 g cm^{-3}, an average detonation velocity of 4500 ms^{-1}, a specific energy of 522 kJ kg^{-1} and a heat energy of 2278 kJ kg^{-1} (www.nitroerg.pl). The explosive material occupied approximately 15 m of each blasthole. The remainder of each blasthole was filled with stemming

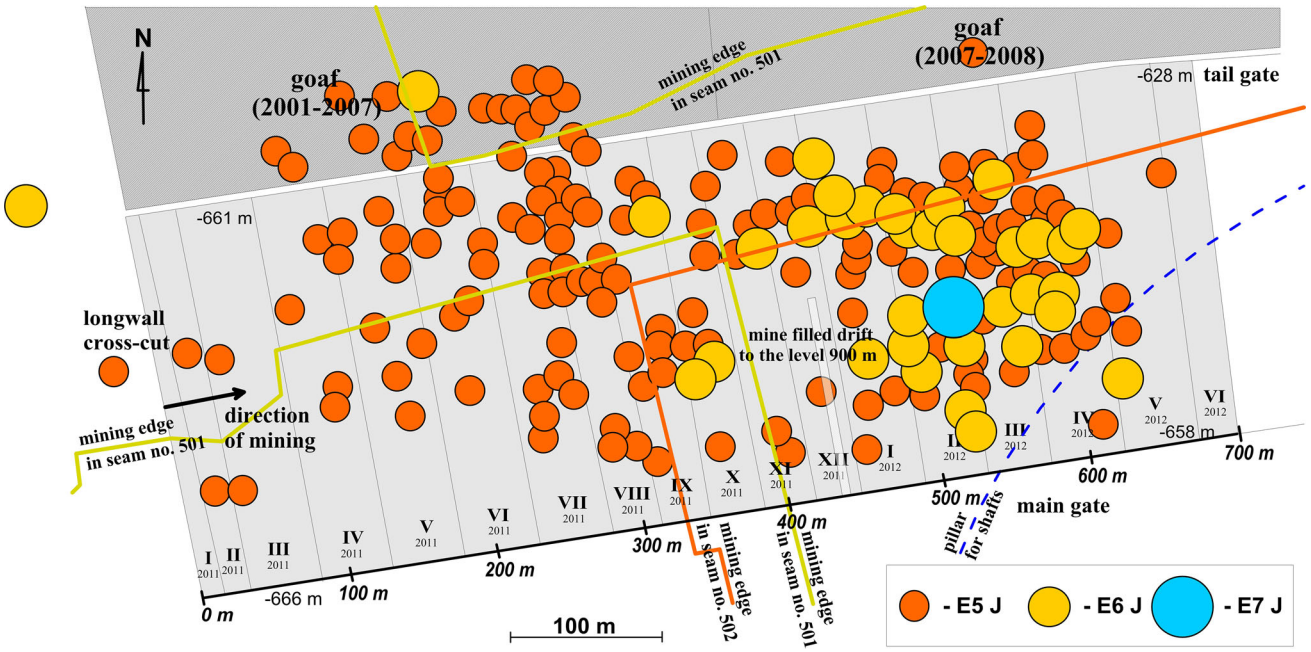

Fig. 2 Location of high-energy tremor sources induced during the longwall mining of coal seam no. 507 with the selected longwall (modified after Wojtecki and Konicek 2016)

(cylindrical paper bags filled with clay and sand). In total, 432 kg of Emulinit PM was detonated during each blasting. Detonation was performed without delay. The blasting stages immediately provoked tremors with the seismic energy range of 3×10^4 J ($M_L = 1.41$) to 9×10^4 J ($M_L = 1.66$). The blasting stages were performed at 25-m intervals of the longwall face advance on average.

Because of the high seismic activity and its correlation with the high level of rockburst hazard near the mining edges in coal seams nos. 501 and 502, which appeared in August 2011, the destress blasting stages were subsequently performed with increased amounts of blasted explosives. Then, 96 kg of the Emulinit PM was loaded in each blasthole. The explosive material occupied almost 20 m of each blasthole length. In each destress blasting stage, 576 kg of explosives was detonated. The blasthole inclination was increased to 40° from the horizon: this value was determined to be optimal for both geological conditions and technical capability. At the end of October 2011, the arrangement of blastholes was accommodated to the locations of the foci of high-energy tremors. During the period of high seismic activity, which lasted till the end of January 2012, 13 destress blasting stages with the above parameters were performed on average at 15-m intervals of the longwall face advance. These blasting stages provoked immediate tremors with the energy of 4×10^4 J ($M_L = 1.47$) to 9×10^4 J ($M_L = 1.66$).

In February 2012, in the area of the selected longwall, a decrease in seismic activity was observed. The lower level of rockburst hazard reduced the frequency of destress blasting from the longwall face. Till then, blasting stages were performed on average at 23-m intervals of the longwall face advance. A stable distribution of blasthole pairs was restored. In this period, nine long-hole destress blasting stages were performed, which provoked immediate tremors with the energy of 4×10^4 J ($M_L = 1.47$) to 8×10^4 J ($M_L = 1.63$).

During the extraction of coal seam no. 507 with the assigned longwall, 33 destress blasting stages were performed from the longwall face. Each long-hole destress blasting stage provoked immediate tremor with the energy of 3×10^4 J ($M_L = 1.41$) to 9×10^4 J ($M_L = 1.66$). In total, 17,424 kg of explosives was blasted, which released 2×10^6 J of seismic energy. The location of the blastholes in the roof rocks (dashes arranged in the "V" letter) and the foci of the provoked tremors are shown in Fig. 3. Monthly longwall face advances (from I 2011 to VI 2012) and the axis along the main gate (from 0 to 700 m) are also shown. The seismic source parameters of the described provoked tremors were analysed.

5 Seismic Source Parameters

This paper is based on a simple well-known model presented by Brune (1970) and developed by Madariaga (1976), who changed the concept of the source radius. The first model assumes a circular dislocation along which an instantaneous stress drop occurs, whereas the second model considers the source as an expanding circular crack with finite rapture velocity; Brune's source radius can be considered approximately twice Madariaga's source radius (Trifu et al. 1995).

Seismic source parameters are always estimated for the seismic events induced in mines [e.g. deep gold mines (McGarr et al. 1989), copper mines (Trifu et al. 1995; Orlecka-Sikora et al. 2012; Lizurek and Wiejacz 2012; Lizurek et al. 2015; Rudzinski et al. 2016) and coal mines (Gibowicz and Kijko 1994; Dubiński et al. 1996)], but it is rare for destress blasting effects (e.g. Srinivasan et al. 2005). Seismic source parameters, which characterize the focus of tremor, are calculated based on the records from seismic stations. The velocity spectra $V(f)$ and displacement spectra $D(f)$ are considered (Kwiatek et al. 2016). By integrating these spectra in the frequency domain, parameters J and K are calculated as follows (Andrews 1986; Snoke 1987; Mendecki 1997):

$$J = 2\int_0^\infty V^2(f)\mathrm{d}f \tag{1}$$

$$K = 2\int_0^\infty D^2(f)\mathrm{d}f \tag{2}$$

where f is the frequency.

However, in practice, both power spectra are calculated for finite frequency limits f_1 and f_2. The low-frequency limit is usually taken as a reciprocal of the duration time of the available data for the Fourier transform. The upper limit is defined based on Nyquist frequency, the sensor or system response, or noise characteristics. This numerical approach underestimates the J and K power spectra, and they must be corrected (Mendecki 1997).

Using parameters J and K (power spectra of the velocity and displacement, respectively), the two basic independent seismic source parameters (low-frequency spectral level Ω_o and corner frequency f_o) are determined as follows (Andrews 1986; Snoke 1987):

$$\Omega_o = 2\left(\frac{K^3}{J}\right)^{\frac{1}{4}} \tag{3}$$

$$f_o = \frac{1}{2\pi}\left(\frac{J}{K}\right)^{\frac{1}{2}} \tag{4}$$

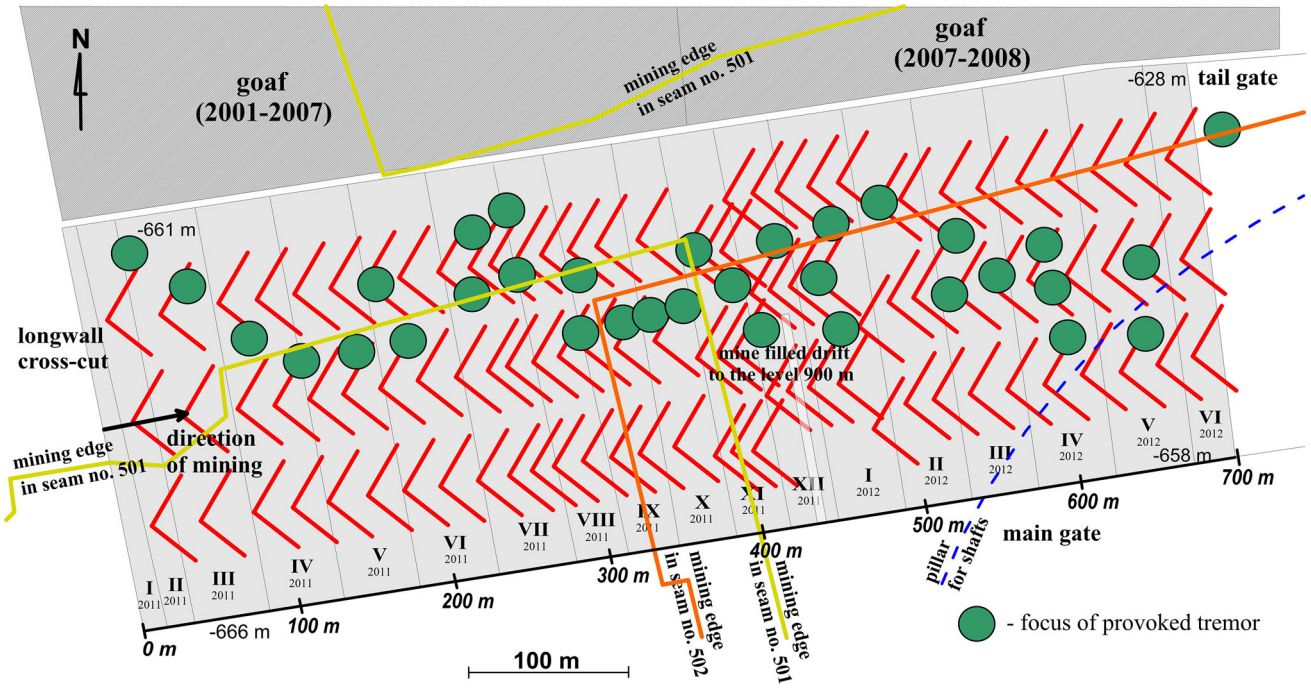

Fig. 3 Location of blastholes drilled from the longwall face and foci of the provoked tremors during the mining of coal seam no. 507 (Wojtecki and Konicek 2016, modified)

The scalar seismic moment M_o most reliably estimates the size of a tremor and can be calculated as follows (Aki and Richards 1980; McGarr et al. 1989; Trifu et al. 1995):

$$M_{\mathrm{o}} = \frac{4\pi\rho V_{\mathrm{c}}^3 R\Omega_{\mathrm{o}}}{R_{\mathrm{c}} F_{\mathrm{c}} S_{\mathrm{c}}} \tag{5}$$

where ρ is the density in the source area, V_{c} is the P- or S-wave velocity in the source area and R is the distance between the source and the receiver. The three components in the denominator denote the correction for the radiation (R_{c}), free-surface effect (F_{c}) and site (S_{c}). The scalar seismic moment of relatively strong events in the mines varies for different induced tremors and depends on the source size and geology conditions. For example, in the deep gold mine, the seismic moments were 9.5–16.2$\times$ 0^{18} Nm for the magnitude of approximately four (M4 event) (McGarr et al. 1989). The relatively weaker induced tremors (magnitude 2–3) in a Canadian copper mine were characterized by smaller M_0, and their moment was 3.4–88.0 $\times$ 10^{15} Nm (Table 1) (Trifu et al. 1995). Furthermore, in Polish copper mines, the stronger tremors of the 3.5–4.5 magnitude produced seismic moments of 5.1–83.4 $\times$ 10^{13} Nm (Table 1) (Orlecka-Sikora et al. 2012; Lizurek et al. 2015; Rudzinski et al. 2016), which is two orders of magnitude less than that in Trifu et al. (1995). The seismic moment was also calculated to be 1.6–81.0 $\times$ 10^{12} Nm for the rockburst events (local magnitude 3–4) in Polish coal mines (Dubiński et al. 1996), whereas Cichowicz (1981) reported tremors from the "Bobrek" Colliery with M_0 = 1–32.5 $\times$ 10^{15} Nm (Table 1). Different characteristics of microtremor events, roof falls and blasts in Indian hard coal mines were reported by Srinivasan et al. (2005). They showed that the seismic moment of the microtremors and roof falls was 1 $\times$ 10^5–4 $\times$ 10^9 Nm, but for the blastings with 400–600 kg of explosives, they observed local magnitudes of −0.6 to 1.2, and the seismic moment changed from 1.2 to 280.0 $\times$ 10^8 Nm (Table 1) (Srinivasan et al. 2005). Interestingly, the presented data were not directly proportional, e.g. 400 kg of explosive in one blasting produced a local magnitude of 0.4 and M_0 = 3.4 $\times$ 10^9 Nm (Table 1), but 563 kg of explosive generated a blast with a local magnitude of −0.6 and M_0 = 1.2 $\times$ 10^8 Nm (Srinivasan et al. 2005).

Scalar seismic moment M_o enables the calculation of moment magnitude M_w (Hanks and Kanamori 1979):

$$M_w = \frac{2}{3}\log_{10} M_o - 6 \tag{6}$$

The moment magnitude is usually smaller than local magnitude M_{L}, which can be found in works considering both values, e.g. Baruah et al. (2012) and Lizurek et al. (2015), and their interdependence may be represented by a simple linear relation. For example, Baruah et al. (2012) showed that natural earthquakes in India produced almost identical values of M_{w} and M_{L}. Otherwise, these magnitudes differed from each other for induced tremors in copper mines according to Lizurek et al. (2015).

Table 1 Comparison of the reported source parameters of the presented authors

References	Type/mine	M_o (Nm)	r (m)	$\Delta\sigma$ (bar)	σ_a (bar)
McGarr et al. (1989)	Induced by mining/gold mine	$9.5–16.2 \times 10^{18}$	236–708	20–317	–
Trifru et al. (1995)	Induced by mining/Canadian copper mine	$3.4–88.0 \times 10^{15}$	39–114	7–61	7–27
Orlecka-Sikora et al. (2012), Lizurek et al. (2015), Rudzinski et al. (2016)	Induced by mining/Polish copper mine	$5.1–83.4 \times 10^{13}$	100–533	–	–
Cichowicz (1981)	Induced by mining/Polish hard coal mine	$1.0–32.5 \times 10^{11}$	25–240	0.3–16	–
Dubiński et al. (1996)	Induced by mining, causing rockburst/Polish hard coal mine	$1.6–81.0 \times 10^{12}$	6–16	5–10	0.5–16
Srinivasan et al. (2005)	Provoked by blastings/Indian hard coal mine	$1.2–280.0 \times 10^{8}$	2–34	3–556	2.3–326

The seismic energy E_c may be determined from the mean average radiation coefficient $\langle R_c \rangle$ according to formula presented by Gibowicz and Kijko (1994):

$$E_c = 4\pi\rho V_c \langle R_c \rangle^2 \left(\frac{R}{F_c R_c}\right)^2 J \tag{7}$$

This parameter characterizes the wave energy emitted from a tremor source. The seismic energy E_c should be calculated separately for P- and S-waves (E_p and E_s, respectively). These energies are calculated differently from the numerical integration method. The E_s/E_p ratio may indicate the nature of dynamic processes in the source. In copper mines, values of S-to-P-wave energy ratio above 20 indicate that the DC (double-couple) component is dominant in the focal mechanism (Król 1998; Lizurek and Wiejacz 2011). Ratio values below 20 indicate that other components of the mechanism solution are also present in the source (Lizurek and Wiejacz 2011). However, Trifu et al. (1995) show lower limit when the energy ratio is approximately 10; for larger ratios, a pure shear failure can be expected.

The source radius r is calculated based on the S-wave velocity V_s and corner frequency f_o, as follows:

$$r = \frac{cV_s}{2\pi f_o} \tag{8}$$

The value of constant c depends on the source model (Brune 1970; Madariaga 1976). In Brune's and Madariaga's source model (Brune 1970; Madariaga 1976), constant c is 2.34 and 1.32, respectively. Madariaga's source radius is commonly two times smaller than Brune's (Trifu et al. 1995). The source radius of mining tremors is close to an exploitation field length (a longwall length) or can inclusion a slip at the level of mining workings in the entire seismic deformation if the event occurs much higher than the mining level (McGarr et al. 1989). Moreover, the rapture area is inversely proportional to the corner frequency, which depends on the rapture process, and if the range of failure scales increases, the rapture process becomes more complex (McGarr et al. 1989). The study in copper mines shows that the source radius of tremors can reach a few hundred metres, e.g. 100–200 m (Cichowicz 1981; Lizurek et al. 2015), 400 and 533 m (Table 1) (Orlecka-Sikora et al. 2012) or 236 and 708 m (Table 1) in a deep gold mine (McGarr et al. 1989). Smaller radii were observed in a coal mine for the rockbursts (Dubiński et al. 1996) of several to a dozen of metres. Moreover, Trifu et al. (1995) reported that in Strathcona copper mine, Canada, the source radii were several dozen metres (50–100 m).

Based on the calculated source radius r, stress drop $\Delta\sigma$ can be determined as follows (Aki and Richards 1980; McGarr et al. 1989; Trifu et al. 1995):

$$\Delta\sigma = \frac{7}{16}\frac{M_o}{r^3} \tag{9}$$

This parameter indicates the difference in stress level before and after the tremor occurs. It strongly depends on the inverse proportion of the source radius of the assumed source model. Worldwide earthquake studies report static stress drop values of 10–50 bar (Trifu et al. 1995). The induced tremors (McGarr et al. 1989; Trifu et al. 1995; Srinivasan et al. 2005) and rockburst events (Dubiński et al. 1996) generally do not deviate from this range, but Cichowicz (1981) reported lower ranges of 0.3–16 bar for tremors from the Bobrek Colliery (Table 1). However, individual tremors with value exceeding 100 bar can be found (e.g. McGarr et al. 1989), which is caused by the extremely large source radius. Moreover, Srinivasan et al. (2005) show that the blasting static stress drop is 3–556 bar (Table 1).

The apparent stress σ_a is the radiated energy per unit area per unit slip. This parameter does not reflect the actual stress drop. It is calculated as follows (Aki and Richards 1980; McGarr et al. 1989; Trifu et al. 1995):

$$\sigma_a = \rho V_s^2 \frac{E}{M_o} = \eta <\sigma> \quad (10)$$

where η is the seismic efficiency and $<\sigma>$ is the average shear stress, which is proportional to the seismic drop. The apparent stress may be considered an independent source parameter (Gibowicz and Kijko 1994).

6 Results

The seismic source parameters were calculated based on seismograms registered by underground seismic stations surrounding the source. Then, the seismograms were integrated to obtain the ground motion spectra. The data set was obtained from a network of 16 seismic stations (Fig. 4) in underground excavations at the depth of 320–1000 m. The network was mainly composed of vertical SPI-70 seismometers and DLM-2001 geophones, which were installed on bolts and vertically oriented. These sensors measured the signals with a minimal frequency of 1 Hz. The upper limit of the transmitted frequencies was 50 Hz. The signals were recorded with a dynamic range less than 72 dB. Each channel had its own amplitude gain. The sampling rate was 5000 samples per second. The timing of the seismological system was synchronized by the global positioning system. The configuration of the seismic network in the seismic monitoring of the investigated longwall in coal seam no. 507 is shown in Fig. 4, where the squares denoted with letter "S" represent the seismic stations.

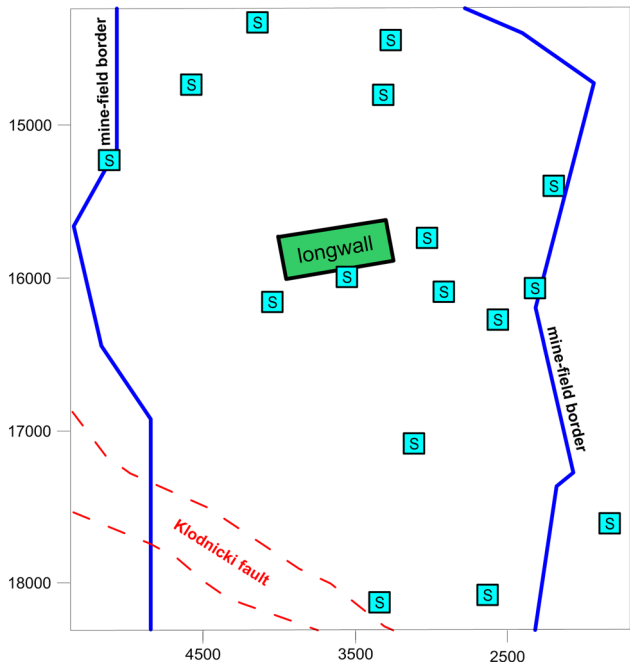

Fig. 4 Configuration of the seismic network around the longwall in coal seam no. 507

The error of the epicentre location was approximately 20–35 m, and the error of the hypocentre location was over 60 m in extreme cases (Kołodziejczyk 2009) but typically smaller. The errors of tremor source locations depend on the number of seismic stations whose data are used in the calculations.

The seismic source parameters were calculated with the FOCI software (Kwiatek et al. 2016). To determine the seismic source parameters, only the data set from the same seismometers was selected. The P- and S-waves were manually marked on the seismograms. Then, the appropriate parts of the seismogram were transformed with the fast Fourier transformation (FFT). The low-frequency spectral level Ω_o and corner frequency f_o were estimated for every spectrum of P- and S-waves. Subsequently, scalar seismic moment M_o, moment magnitude M_w, seismic energy E_c, source radius r (according to Brune's source model), stress drop $\Delta\sigma$, apparent stress σ_a and S-to-P-wave energy ratio were calculated. Calculations were done for each seismic station after each blasting. The calculated seismic source parameters were averaged for each provoked tremor. The averaged seismic source parameters of each provoked tremor are listed in Table 2. Because of the averaged values, the above formulas cannot be directly applied.

By analysing the mining history with the described longwall, the recorded pattern of seismic activity and calculated seismic source parameters of provoked tremors (particularly ratio E_s/E_p), one can distinguish three groups of tremors: group 1: tremors 1–10; group 2: tremors 11–27; group 3: tremors 28–33. The averaged values of seismic source parameters in each group are listed in Table 2.

Tremors 1–10 were provoked in the beginning of the longwall mining and before the longwall face had reached the area where the mining edges in the upper seams (nos. 501 and 502) were quasi-parallel to the longwall face. Blasting stages 1–10 had identical parameters.

The average ratio E_s/E_p in this group is low (mean value: 2.8) and indicates the domination of the non-shear mechanism (Trifu et al. 1995; Lizurek and Wiejacz 2011; Wojtecki et al. 2016). The rock mass fracturing was mainly caused by the detonation of explosives, and the shear mechanism component was small, as confirmed by the seismic moment tensor inversion method (Wojtecki et al. 2013).

The second group includes tremors that were generally provoked when the longwall face ran beneath the mining edges in the upper coal seams (nos. 501 and 502) and were

Table 2 List of the calculated and averaged seismic source parameters of tremors provoked by destress blastings

No.	Date	Time		Weight of explosives (kg)	Seismic source parameters								
		h	min		Ω_o (10^{-8})	f_o (Hz)	M_o (10^{10} Nm)	M_w	E (10^5 J)	r (m)	$\Delta\sigma$ (10^6 Pa)	σ_a (10^4 J/m^3)	$\frac{E_s}{E_p}$
1.	2011-02-14	5	44	432	5.05	24.05	16.2	1.19	1.17	39.4	1.99	4.75	1.3
2.	2011-03-21	6	13	432	13.3	21.94	22.1	1.31	3.46	45	2.35	7.27	4.1
3.	2011-04-04	5	41	432	7.83	19.13	18.0	1.33	1.73	41.3	1.42	3.27	1.5
4.	2011-04-18	6	30	432	6.29	19.7	11.5	1.26	1.48	37.7	1.65	3.44	1.0
5.	2011-05-02	3	30	432	15.6	12.95	19.6	1.43	1.61	56.5	0.61	1.15	5.6
6.	2011-05-16	12	6	432	13.1	15.57	18.2	1.41	1.85	49.8	1.22	1.64	2.5
7.	2011-05-30	7	28	432	4.81	18.94	9.82	1.24	1.35	37.5	1.14	2.49	5.5
8.	2011-06-13	2	34	432	7.07	21.31	13.4	1.33	1.99	38.3	2.51	3.68	1.3
9.	2011-06-27	5	16	432	12.3	16.75	16.6	1.35	1.17	50.8	0.97	1.62	2.6
10.	2011-07-11	5	16	432	6.89	17.12	13.2	1.32	2.03	40.8	1.12	2.23	2.6
Mean					*9.2*	*18.7*	*15.9*	*1.3*	*1.8*	*43.7*	*1.5*	*3.2*	*2.8*
Standard deviation					*3.7*	*3.1*	*3.6*	*0.1*	*0.6*	*6.2*	*0.6*	*1.7*	*1.6*
Minimum					*4.81*	*12.95*	*9.82*	*1.19*	*1.17*	*37.5*	*0.61*	*1.15*	*1.0*
Maximum					*15.6*	*24.05*	*22.1*	*1.43*	*3.46*	*56.5*	*2.51*	*7.27*	*5.6*
11.	2011-07-18	7	7	432	6.57	22.56	10.7	1.28	4.85	36	3.05	7.76	9.0
12.	2011-08-01	5	16	576	43.3	16.58	32.0	1.41	3.38	63.6	1.10	3.05	7.3
13.	2011-08-21	17	56	576	43.7	16.06	28.4	1.45	3.31	58.8	1.34	3.00	6.7
14.	2011-09-04	18	59	576	23.9	15.92	21.8	1.41	2.43	59.4	1.11	2.78	6.9
15.	2011-09-19	5	29	576	46.5	11.53	68.0	1.63	4.83	94.8	0.89	1.83	6.2
16.	2011-10-10	5	48	576	40.3	12.85	48.1	1.62	6.04	61.8	1.16	2.11	5.3
17.	2011-10-30	23	26	576	63.9	12.34	57.7	1.66	5.44	76.4	0.89	1.67	6.9
18.	2011-11-14	0	10	576	43.5	12.97	38.5	1.6	5.14	67.7	1.06	2.08	6.9
19.	2011-11-20	23	16	576	44.1	9.43	32.5	1.6	4.16	71.6	0.59	1.33	7.3
20.	2011-11-28	0	4	576	45.4	9.09	83.5	1.78	8.35	86.5	1.00	2.40	5.5
21.	2011-12-11	23	9	576	51.1	11.45	58.1	1.67	4.75	85.6	1.03	2.40	6.4
22.	2011-12-26	22	43	576	74.3	9.44	38.1	1.53	5.44	69.3	0.66	2.76	7.6
23.	2012-01-08	22	50	576	34.6	12.9	36.9	1.44	3.92	59.7	0.82	2.45	6.2
24.	2012-01-22	23	33	576	51.4	12.42	34.3	1.5	3.39	62.6	0.69	1.58	5.3
25.	2012-02-13	6	28	576	27.3	14.02	48.2	1.43	1.87	74	0.80	2.25	4.5
26.	2012-02-27	5	11	576	28.0	14	26.1	1.46	2.05	61.1	0.86	1.54	4.0
27.	2012-03-12	0	32	576	38.7	12.07	22.7	1.43	2.52	61	0.58	1.48	4.9
Mean					*41.6*	*13.3*	*40.3*	*1.5*	*4.2*	*67.6*	*1.0*	*2.5*	*6.3*
Standard deviation					*14.9*	*3.2*	*17.9*	*0.1*	*1.6*	*13.1*	*0.5*	*1.4*	*1.2*
Minimum					*6.57*	*9.09*	*10.7*	*1.28*	*1.87*	*36*	*0.58*	*1.33*	*4*
Maximum					*74.3*	*22.56*	*83.5*	*1.78*	*8.35*	*94.8*	*3.05*	*7.76*	*9*
28.	2012-03-26	6	29	576	8.73	12.95	17.8	1.35	1.33	52.6	0.57	1.39	2.3
29.	2012-04-09	11	40	576	21.7	12.21	18.9	1.43	3.02	49.8	0.76	2.15	3.3
30.	2012-04-22	23	41	576	42.3	12.24	27.1	1.48	2.46	61	0.67	1.46	3.6
31.	2012-05-06	23	57	576	28.7	16.89	15.6	1.28	1.66	50	0.91	2.57	4.8
32.	2012-05-20	22	51	576	15.5	12.22	11.8	1.32	1.43	49.9	0.52	1.45	3.5
33.	2012-06-03	23	23	576	7.40	16.76	8.09	1.18	0.51	48.1	0.56	1.11	4.2
Mean					*20.7*	*13.9*	*16.5*	*1.34*	*1.74*	*51.9*	*0.7*	*1.7*	*3.6*
Standard deviation					*12.1*	*2.1*	*6*	*0.1*	*0.8*	*4.3*	*0.1*	*0.5*	*0.8*
Minimum					*7.4*	*12.21*	*8.09*	*1.18*	*0.51*	*48.1*	*0.52*	*1.11*	*2.3*
Maximum					*42.3*	*16.89*	*27.1*	*1.48*	*3.02*	*61*	*0.91*	*2.57*	*4.8*

quasi-parallel to the longwall face, which affected the stress level in the rock mass and increased the rock burst hazard (tremors 11–27). Blasting stage no. 11 had identical parameters to those in the first group, but it was performed in a close vertical distance from the mining edges in coal seams nos. 501 and 502. Subsequent blasting stages were performed with a larger amount of explosives.

Some seismic source parameters in the second group have larger average values than in the first group: scalar seismic moment M_o (relative change of approximately 160%), seismic energy E_c (relative change of approximately 133%) and source radius r (relative change of approximately 55%). However, the average low-frequency spectral level Ω_o is higher (relative change of approximately 350%), and the average corner frequency f_o in the second group is lower with a relative change of approximately 29% than those in the first group. The average ratio E_s/E_p in the second group is 6.3, which indicates a shear mechanism under the conditions of hard coal mines (Wojtecki et al. 2016). The highest value of ratio E_s/E_p in this group is 9 (Table 2). The occurrence of shear mechanisms in these foci was confirmed using the seismic moment tensor inversion method (Wojtecki et al. 2013).

Tremors 28–33 in the third group were provoked when the longwall had approached its end and the protecting pillar for the shafts. The final six blasting stages were performed with a large amount of explosives but at a large vertical distance from the mining edges in coal seams nos. 501 and 502.

The average seismic source parameters in the third group are lower than those in the second group: low-frequency spectral level Ω_o (relative change of approximately −50%), scalar seismic moment M_o (relative change of approximately −59%), seismic energy E_c (relative change of approximately −59%) and source radius r (relative change of approximately −23%). The average corner frequencies f_o in these two groups are similar, but the average ratio E_s/E_p in the third group is 3.6, which decreases by approximately 43% compared to the second group. The ratio E_s/E_p generally decreases, which indicates the dominant non-shear mechanism in the tremor source. The obtained results are consistent with the seismic moment tensor inversion method results (Wojtecki et al. 2013). In the foci of these tremors, the explosion mechanism predominated (Wojtecki et al. 2013). The average seismic source parameters in this group are notably similar to those in the first group (scalar seismic moment M_o; moment magnitude M_w; seismic energy E_c) or are higher (low-frequency spectral level Ω_o with a relative change of approximately 125%; source radius with relative change of approximately 19%). The ratio E_s/E_p in the third group is approximately 29% higher than that in the first group but remains low.

The first and second groups had the largest average stress drop $\Delta\sigma$ and average apparent stress σ_a; the third group had smaller average values of these parameters. Tremor no. 11 had the largest stress drop $\Delta\sigma$ and apparent stress σ_a (Table 2).

The variability of the selected seismic source parameters of provoked tremors (E_c, E_s/E_p, M_o and r) during the longwall mining of coal seam no. 507 with selected longwall is shown in Fig. 5. The graphs were constructed using discrete data from each of the 33 blasting stages (the dots have different colours to indicate that they belong to groups 1, 2 or 3). The source parameters of provoked tremors were set in relation to the current position of the longwall. The location of the longwall face during each blasting was calculated after the main gate (Fig. 3). "0" on the horizontal scales in Fig. 5 denotes the location of the longwall cross-cut. The location of mining edges in upper coal seams nos. 501 and 502, which were quasi-parallel to the longwall face, is also shown in Fig. 5. Some seismic source parameters clearly increased when the longwall face ran beneath these mining edges. Therefore, it can be assumed that the blasting stages in the area of coexisting mining edges in coal seams nos. 501 and 502, which were parallel to the longwall face, provoked other processes in the rock mass in addition to the pure explosion caused by detonation.

7 Conclusions

The seismic source parameters describe the foci of tremors. These parameters can also be determined for provoked tremors. The seismic source parameters were calculated for the tremors provoked by the long-hole destress blasting stages during the underground mining of coal seam no. 507 in a hard coal mine in the Polish part of the USCB. The main purpose of these blasting stages was to destress the rock mass ahead of the selected longwall face.

Among 33 foci of the provoked tremors, three groups were distinguished according to the ratio E_s/E_p. The data of group 2, which were obtained while mining under mining edges in coal seams nos. 501 and 502, are generally different from those of groups 1 and 3.

The second group had larger average values of some seismic source parameters than the other groups: low-frequency spectral level Ω_o, scalar seismic moment M_o, moment magnitude M_w, seismic energy E_c and source radius r. The second group had a lower average corner frequency f_o than the other groups. During the extraction of coal seam no. 507, under the effect of the mining factors, which increased the stress in the roof rocks (when the level of the rockburst hazard was the highest), the average ratio E_s/E_p in the second group of tremors was 6.3 (maximally

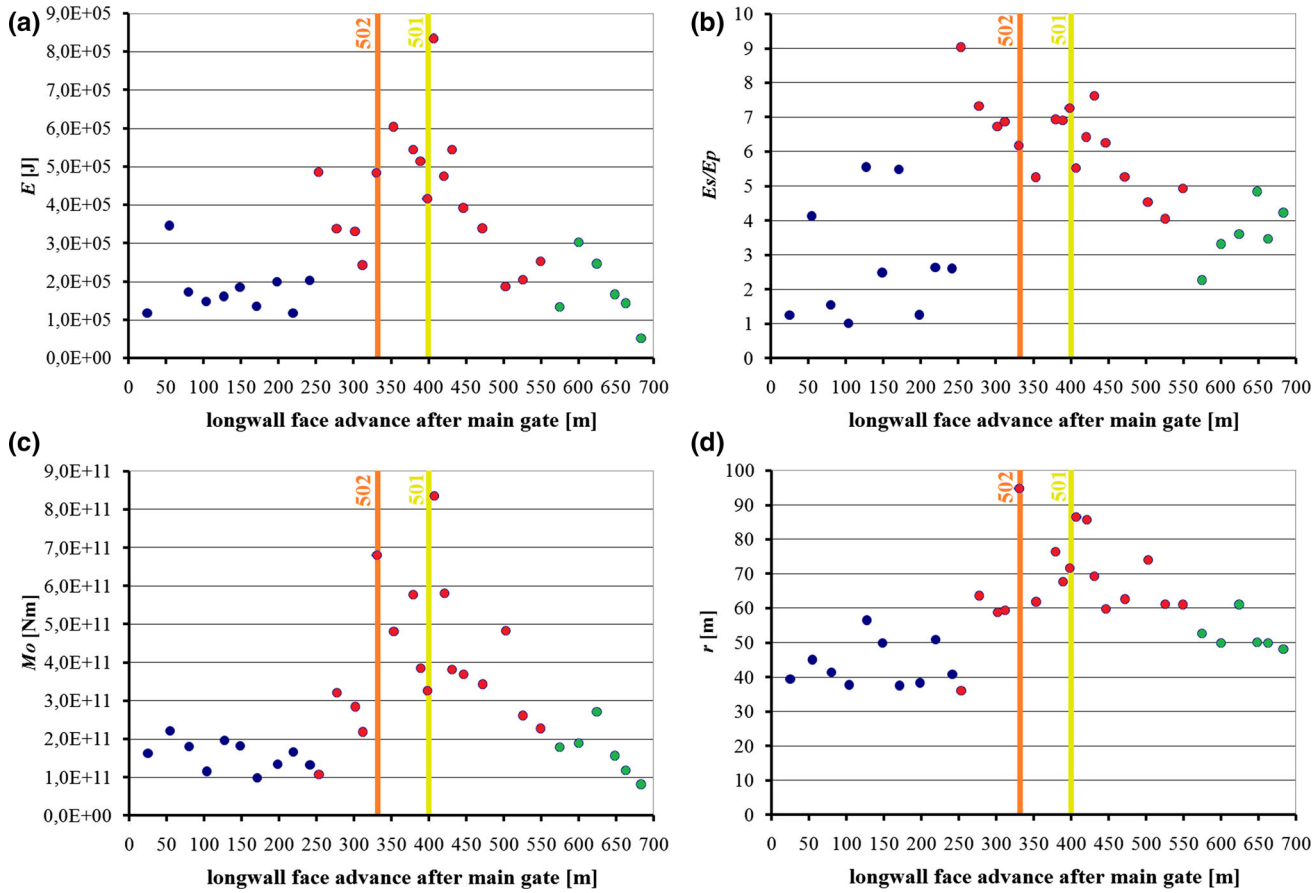

Fig. 5 Changeability of the selected seismic source parameters of the provoked tremors during the longwall mining of coal seam no. 507 with the selected longwall

9), which indicates some share of the shear mechanism in the source under the conditions in hard coal mines (Wojtecki et al. 2016). According to the seismic moment tensor inversion method (Wojtecki et al. 2013), in the second group of tremors, the shear mechanism (reverse slip mechanism) was predominant or clearly distinguished.

In the first and third groups of provoked tremors, the average ratio E_s/E_p was 2.8 and 3.6, respectively. In the absence of additional stresses or when the stress level decreased, the roof rocks fractured in the destress blasting stages mainly because of the detonation of explosives (Wojtecki et al. 2013), which reflects in the values of some seismic source parameters.

The first and second groups of provoked tremors had the largest average stress drop $\Delta\sigma$ (1.5×10^6 Pa and 1.1×10^6 Pa, respectively). The second group had the largest average source radius r among the three groups, which indicates the largest range of stress drop.

From this viewpoint, the destress blasting stages in the roof rocks from the longwall face were more effective when the longwall face was running under the mining edges in the neighbouring seams nos. 501 and 502, which were quasi-parallel to the longwall face. This hypothesis was proven by the lack of high-energy tremors within a short distance from the longwall face. On average, the foci of the high-energy tremors were localized at approximately 90 m on front of the longwall face. The roof rocks of coal seam no. 507 near the longwall face were effectively destressed by the blasting stages. They initiated the processes that led to a new advantageous stress equilibrium in the rock mass, and an elastic strain energy was not accumulated. The effectiveness of the performed destress blasting stages is also confirmed by the lack of destructive effects in the openings in coal seam no. 507, which occurred when destress blasting was not designed.

Established in August 2011, the amount of explosives (96 kg per blasthole) was maintained at a constant level till the end of the active rockburst prevention, which included a period when the longwall face was running under the mining edges in coal seams nos. 501 and 502 and a subsequent period. The provoked tremors in the second and third groups have different seismic source parameters. The first and third groups also have different seismic source parameters, which could partially be caused by the different amounts of explosives.

The seismic source parameters of the provoked tremors provide information about their foci and the processes that

occur within them. It can be determined whether in the focus of a provoked tremor a slip mechanism, correlated with the rock mass achieving a new equilibrium state, is present or not. All of this information can be useful in designing the active rockburst prevention. According to the calculated seismic source parameters after each blasting stage, the parameters of the next blasting stages (location of blastholes, inclination and length of the blastholes, amount of explosives, etc.) can be modified and controlled. The blasting parameters can be adapted to the current situation by analysing the seismic source parameters to maximize the destress effect. The range and magnitude of the destress are particularly important while mining under difficult geological and mining conditions with the high level of rockburst hazard.

An analysis of the seismic source parameters can assist the planning of the blasting parameters. However, further investigations are required under different geological and mining conditions with other blasting parameters. The relationships between the blasting parameters and the seismic source parameters should be specified, and the condition under which the shear mechanism appears should be more precise.

Acknowledgements The project was partially granted by the Centre for Polar Studies, University of Silesia, Poland—The Leading National Research Centre (KNOW) in Earth Sciences 2014–2018 (funded by the National Science Centre granted under Decision No UMO-2012/05/N/ST10/03943) and Young Scientist Program "Seismic Network of the University of Silesia" (1 M-0416-001-1-01).

References

Aki K, Richards PG (1980) Quantitative Seismology. Theory and Methods. Freeman, San Francisco

Andrews DJ (1986) Objective determination of source parameters and similarity of earthquakes of different size. In Das S, Boatwright J, Scholz CH (eds) Earthquake Source Mechanics, Am. Geophys. Union, Washington, D.C., 6:259–267

Baruah S, Baruah S, Bora PK, Duarah R, Kalita A, Biswas R, Gogoi N, Kayal JR (2012) Moment magnitude (M W) and local magnitude (M L) relationship for earthquakes in Northeast India. Pure appl Geophys 169(11):1977–1988

Brune JN (1970) Tectonic stress and the spectra of seismic shear waves from earthquakes. J Geophys Res 75:4997–5009

Cichowicz A (1981) Determination of source parameters from seismograms of mining tremors and the inverse problem for a seismic source. Publications of the Institute of Geophysics of PAS 11, Państwowe Wyd. Nauk. (**in Polish**)

Dubiński J, Wierzchowska Z (1973) Methods for the calculation of tremors seismic energy in the Upper Silesia. Research Works of Central Mining Institute, 591, Katowice (**in Polish**)

Dubiński J, Mutke G, Stec K (1996) Focal mechanism and source parameters of the rockburst in Upper Silesian Coal Basin. Acta Mont IRSM AS CR 9(100):17–26

Gibowicz SJ, Kijko A (1994) An introduction to mining seismology. Academic Press, San Diego

Hanks TC, Kanamori H (1979) A moment magnitude scale. J Geophys Res 84:2348–2350

Kołodziejczyk P (2009) Optimization of the Seismic Network in Kompania Węglowa S.A. Gliwice (**in Polish**, not published)

Konicek P, Soucek K, Stas L, Singh R (2013) Long-hole destress blasting for rockburst control during deep underground coal mining. Int J Rock Mech Min Sci 61:141–153

Król M (1998) Zastosowanie tensora momentu sejsmicznego oraz analizy widmowej fal sejsmicznych do badania ognisk wstrząsów z rejonu kopalni miedzi "Polkowice-Sieroszowice". Dissertation, Institute of Geophysics, Polish Academy of Sciences, Warsaw (**in Polish**, not published)

Kwiatek G, Martínez-Garzón P, Bohnhoff M (2016) HybridMT: A MATLAB/shell environment package for seismic moment tensor inversion and refinement. Seismol Res Lett. doi:10.1785/0220150251

Lizurek G, Wiejacz P (2011) Moment tensor solution and physical parameters of selected recent seismic events at Rudna Copper Mine. In: Idziak AF, Dubiel R (eds) Geophysics in mining and environmental protection, geoplanet: earth and planetary sciences, vol 2. Springer, Berlin, pp 11–19

Lizurek G, Rudziński Ł, Plesiewicz B (2015) Mining induced seismic event on an inactive fault. Acta Geophys 63(1):176–200

Madariaga R (1976) Dynamics of an expanding circular fault. Bull Seismol Soc Am 66:639–666

McGarr A, Bicknell J, Sembera E, Green RWE (1989) Analysis of exceptionally large tremors in two gold mining districts of South Africa. Pure Appl Geophys 129(3/4):295–307

Mendecki AJ (1997) Seismic monitoring in mines. Chapman and Hall, London

Orlecka-Sikora B, Lasocki S, Lizurek G, Rudziński Ł (2012) Response of seismic activity in mines to the stress changes because of mining induced strong seismic events. Int J Rock Mech Min Sci 53:151–158

Rudziński Ł, Cesca S, Lizurek G (2016) Complex rupture process of the 19 March 2013, Rudna Mine (Poland) induced seismic event and collapse in the light of local and regional moment tensor inversion. Seismol Res Lett 87(2A):274–284

Snoke JA (1987) Stable determination of (Brune) stress drops. Bull Seismol Soc Am 64:1295–1317

Srinivasan C, Sivakumar C, Gupta RN (2005) Source parameters of seismic events in a coal mine in India. In: Proceedings of 27th Seismic Research Review: Ground-Based Nuclear Explosion Monitoring Technologies, pp 653–662

Trifu CI, Urbancic TI, Young RP (1995) Source parameters of mining-induced seismic events: an evaluation of homogeneous and inhomogeneous faulting models for assessing damage potential. Pure Appl Geophys 145(1):3–27

Wojtecki Ł, Dzik G (2013) Characteristics of the focal mechanism of high-energy tremors occurring during longwall mining of coal seam 507. Przegląd Górniczy 12:17–22 **(in Polish)**

Wojtecki Ł, Konicek P (2016) Estimation of active rockburst prevention effectiveness during longwall mining under disadvantageous geological and mining conditions. J Sustain Min (in print)

Wojtecki Ł, Talaga A, Mendecki MJ, Zuberek MW (2013) The estimation of the torpedo blasting effectiveness based on the analysis of the focal mechanisms of induced mining tremors in Bielszowice Coal Mine. In: Kwaśniewski M, Łydźba D (eds)

Rock mechanics for resources, energy and environment. Taylor and Francis Group, London, pp 769–774
Wojtecki Ł, Mendecki MJ, Zuberek WM (2016) An attempt to determine the seismic moment tensor of tremors induced by destress blasting in coal seam. Int J Rock Mech Min Sci 83:162–169. http://www.nitroerg.pl/en/products/emulinit-pm.html